Received: 19 February 2019

DOI: 10.1002/mop.31873

WILEY

RESEARCH ARTICLE

# A 16-modified antipodal Vivaldi antenna array for microwave-based breast tumor imaging applications

**Md Samsuzzaman**[1,2] | **Mohammad T. Islam**[1] | **Md T. Islam**[1] | **Abdullah A. S. Shovon**[2] | **Rashed I. Faruque**[3] | **Norbahiah Misran**[1]

[1]Faculty of Engineering and Built Environment, Universiti Kebangsaan Malaysia, Bangi Selangor, Malaysia

[2]Patuakhali Science and Technology University, Patuakhali, Bangladesh

[3]Space Science Centre (ANGKASA), Universiti Kebangsaan Malaysia, Bangi, Selangor Malaysia

**Correspondence**
Md Samsuzzaman, Faculty of Engineering and Built Environment, Universiti Kebangsaan Malaysia, Bangi Selangor, Malaysia.
Email: samsuzzaman@siswa.ukm.edu.my

**Funding information**
Universiti Kebangsaan Malaysia

**Abstract**

In this article, an improved method is introduced for enhancing the gain and directivity of a modified antipodal Vivaldi antenna, which is suitable for detecting malignant cells in the breast through microwave imaging. By slotting on the fins of the antenna with the addition of parasitic elliptical patch makes the antenna radiation more directive with more gain at the lower band range. The operating fractional bandwidth of this proposed Vivaldi antenna is 120% (2.50-11 GHz) with compact dimension and directive radiation pattern with 7.20 dBi highest gain. The antenna time-domain performance and the near-field directivity (NFD) are also observed. Effective microwave breast phantom imaging system with an array of 16 antipodal antennas is designed where one antenna works as a transmitter and rest of the antenna works as a receiver in turn. The imaging performance is investigated with tumor inside the breast phantom using the Microwave Radar-Based Imaging Toolbox open source software. Detection of tumor tissue inside breast phantom has been identified by analyzing the modified antipodal Vivaldi antennas' backscattered signal.

**KEYWORDS**

antipodal Vivaldi antenna, breast tumor, microwave imaging, parasitic elliptical patch

## 1 | INTRODUCTION

Breast tumor is an abnormal mass of tissue or swelling in a breast, which can be a benign or cancerous (malignant) cell. Nowadays, breast cancer is considered one of the major health issues across the globe, which develops from breast tissue (malignant tissue). About 25% of cases of cancers among women are accountable for breast cancer globally each year.[1] Present days, microwave imaging (MI) is a promising method for screening the human body to identify abnormality relying on the electrical properties of healthy and malignant tissues. MI is becoming more popular for its low cost, complexity, and non-ionizing effects. It also offers high data rate to reconstruct better resolution images. Still, it is challenging to establish a suitable system to be used in screening. The antenna acts as a transceiver in the MI system. To get accurate results, the antenna should be highly efficient and possess good radiation characteristics. The Vivaldi antenna is a good candidate in this race for its directionality, high gain, and better impedance matching. It can achieve high gain without compromising the size.

Numerous antennas are designed over time for breast phantom imaging, such as pyramidal horn antenna,[2] the Vivaldi antenna,[3–5] CPW antenna,[6] EBG antenna and metamaterials,[7] array antenna,[8] and the slotted antenna.[9–12] The main difficulty of designing an antipodal Vivaldi antenna is to get a directive radiation pattern and a lower frequency band resonance with compact dimension. From 1987, Vivaldi antenna design has given much consideration for medical applications for the identical properties that are desired for microwave imaging.[13,14] For enhancing the performance, several researchers have introduced different methods with new techniques in the lower frequency such as tapered slot,[15] planar directors,[16] exponential slot edged,[17] loaded with parasitic ellipse in the patch,[18] bending feed,[19] cavity-backed,[20] fern leaf-type fractal layout,[21] side slotted fin,[4,22] artificial material lens and reflector,[23] and corrugated Vivaldi.[3] The tapered slot technique was introduced to achieve directional radiation in a square-shaped Vivaldi antenna with limited bandwidth (BW).[15] An enhanced Vivaldi antenna was

  

designed having planar directors in the aperture end to increase directivity through large dimension.[16] A palm tree structure was anticipated to attain end-fire radiation through exponential slot edge, but not to achieve lower frequency impedance band and higher gain.[17] A parasitic ellipse has added into the patch to increase the performance of the designed Vivaldi antenna through filed coupling with large dimension.[18] Bending feed line structure and tapered slot were introduced in the antipodal Vivaldi antenna for microwave imaging application with a small size to increase operational BW, but the gain and efficiency are less than 5dBi and 70%, correspondingly.[19] For breast phantom screening, a cavity back Vivaldi was designed to enhance the antenna performance with compact dimension and low gain.[20] To achieve high-performance antenna properties, a fern leaf-type fractal layout antenna was proposed just for imaging applications.[21] A complex structure and the low-gain antipodal antenna were designed to achieve wide impedance BW.[22] A corrugated multiple slotted Vivaldi was designed to enhance the antenna performance for MI application with a big object.[3] Besides, compact antipodal Vivaldi antenna loaded with tapered slot, an artificial material lens, and reflector for GPR application with large dimension 430 mm × 280 mm.[23] So, the compact antenna with improved properties is anticipated for MI applications.

In this article, the design and application of modified Vivaldi antenna in microwave breast imaging system are offered. The antenna has wide BW and good gain with directional radiation patterns. The numerical and experimental results of the antenna are investigated. An array of 16 antennas is used in an imaging setup for breast phantom imaging to identify the tumor inside the phantom successfully using Microwave Radar Based Imaging Toolbox (MERIT) open-source software imaging tool. The simulation setup and imaging results are also presented.

## 2 | ANTENNA LAYOUT DESIGN

The main purpose of the designing the antenna is to categorize the difference in dielectric constant between the healthy and malignant breast tissues. For considerably high-resolution image and better penetration, numerous resonance frequencies are essential at the resonant part of the breast.[20] Lower frequency resonance, high gain, and directive radiation are highly required for MI. Vivaldi antennas are most suited for its good to gain, directionality in radiation, and higher pulse converging peak values. It offers a narrow pulse width besides constant

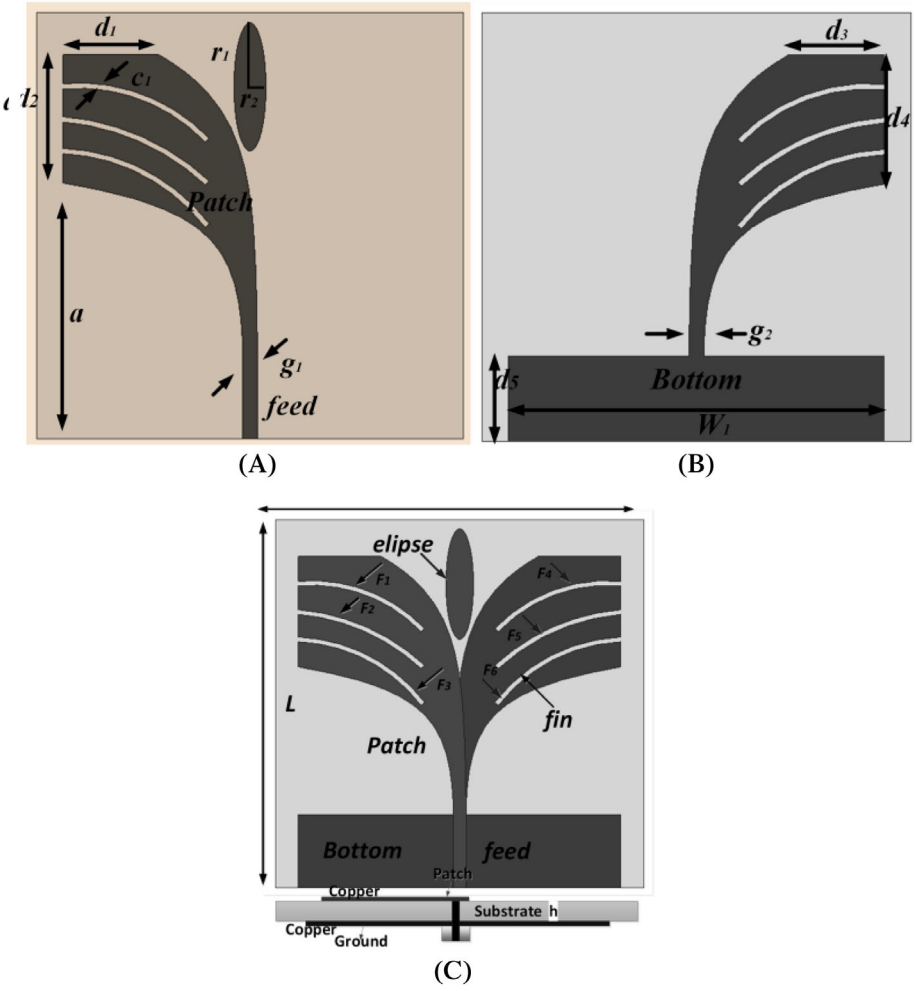


**FIGURE 1** Design layout: A, top, B, bottom, and C, overall perspective [Color figure can be viewed at wileyonlinelibrary.com]

group delay. The geometry of the designed antenna can be found in Figure 1A as top, Figure 1B as bottom, and Figure 1C as an overall perspective. Epoxy resin fiber (FR4) is used as the dielectric substrate with 1.6 mm height, the dielectric constant of 4.4, and the tangent loss of 0.02. The designed antenna has modified patch and ground plane with an elliptical parasitic element as main radiating parts and was fed with a 50-Ω feed line. These elements are adjusted in such a way to achieve the desired antenna performance. Irregular slots and elliptical extension are inspected to enhance the electrical length to reach the lower band. The inner and outer sides of the tapered form are evaluated by

$$x_i = \pm c_s \cdot \exp(k_s y) \mp (c_s + 0.5 \cdot c_w) \quad (1)$$

$$x_0 = \pm c_w \cdot \exp\left(k_w y^{sf}\right) \mp (c_s + 0.5 \cdot c_w) \quad (2)$$

where $x_i$ and $x_0$ both represent the distance from the slot center to the inner and outer boundaries, exclusively.[24] The endpoint frequency of the antenna is calculated by the following equation:[25]

$$f_r = \frac{c}{\left[w' \sqrt{(\varepsilon_r)}\right]} \quad (3)$$

where $f_r$ stands for resonant frequency, $c$ expresses the speed of light, $w'$ represents the thickness of the beginning edge, and $\varepsilon_r$ is the relative permittivity of the prototype material. To enhance the BW, three widths of 0.5 mm have been cut from both the fins. These cuts and ellipse have a significant effect on the surface current distribution that helps to achieve a lower frequency band. A partial rectangular slot has been cut out at the bottom of the ground with the altitude of $d_5$ for balancing the Vivaldi antenna. Table 1 demonstrates the final design parameters of the proposed antenna.

**TABLE 1** Realized antenna parameter

| Parameters | mm | Parameters | mm |
|---|---|---|---|
| $L$ | 40 | $g1$ | 1.4 |
| $W$ | 40 | $g2$ | 1.4 |
| $W1$ | 35 | $C1$ | 8 |
| $d1$ | 9 | $r1$ | 6 |
| $d2$ | 12 | $r2$ | 1.5 |
| $d3$ | 9 | $a$ | 24 |
| $d4$ | 12 | $h$ | 1.6 |
| $d5$ | 8 | | |

The surface magnitude current distribution of the optimized antenna at various frequencies of 3.3 and 7.0 GHz is shown in Figure 2A,B, respectively. Most of the current is conducting through the radiating fins, around the cutting slots and ellipse. The current is well distributed accompanied by the top and bottom radiators at low frequencies. Several null values are typical at the higher band due to the higher-order current mode penetration. The current ways change because of the presence of the slots that generate a higher order current mode. Antenna performance is greatly affected by this characteristic. Concurrently, the gain in the main lobe was enhanced, and the radiation pattern remarkably expands. The slots and ellipse help to avoid tapping. Consequently, the control over current distribution is reestablished to the head-to-head edges of the antenna.

## 2.1 | Parametric study

The proposed antenna includes the patch and ground fronting 180° to each other. The rectangular plane devoted to the ground having the length and width symbolized by $W_1$ and $d_5$ to balance the antenna is shown in Figure 1. Six slots have been cut out from the top and bottom radiators designated by $F_1$, $F_2$, $F_3$, $F_4$, $F_5$, and $F_6$. There is a substantial effect of the slots and elliptical notch on antenna results. Figure 3 represents two tunings on a patch of the elementary antenna, which are labeled as follows: antenna 1 (Ref. 4) and antenna 2 (proposed design with an ellipse) and their reflection coefficient and peak gain result. Initially, the slots etched from both top and bottom radiators at identical

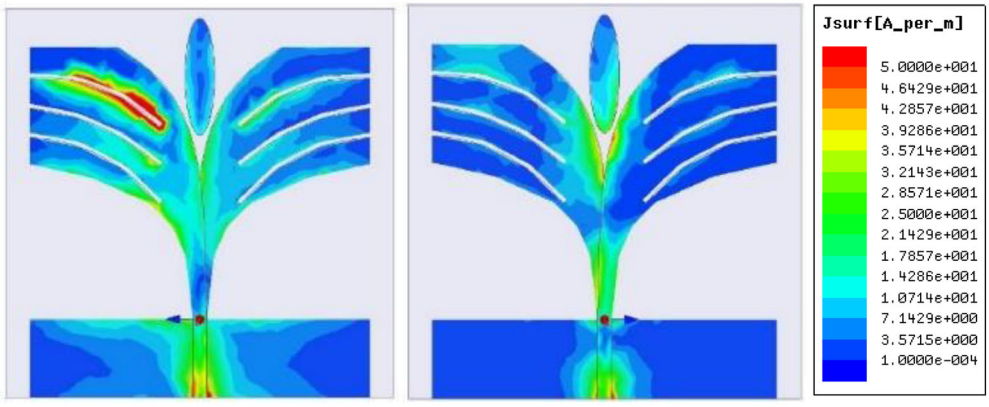


**FIGURE 2** Surface magnitude current distribution: A, 3.30 GHz. B, 7.0 GHz [Color figure can be viewed at wileyonlinelibrary.com]

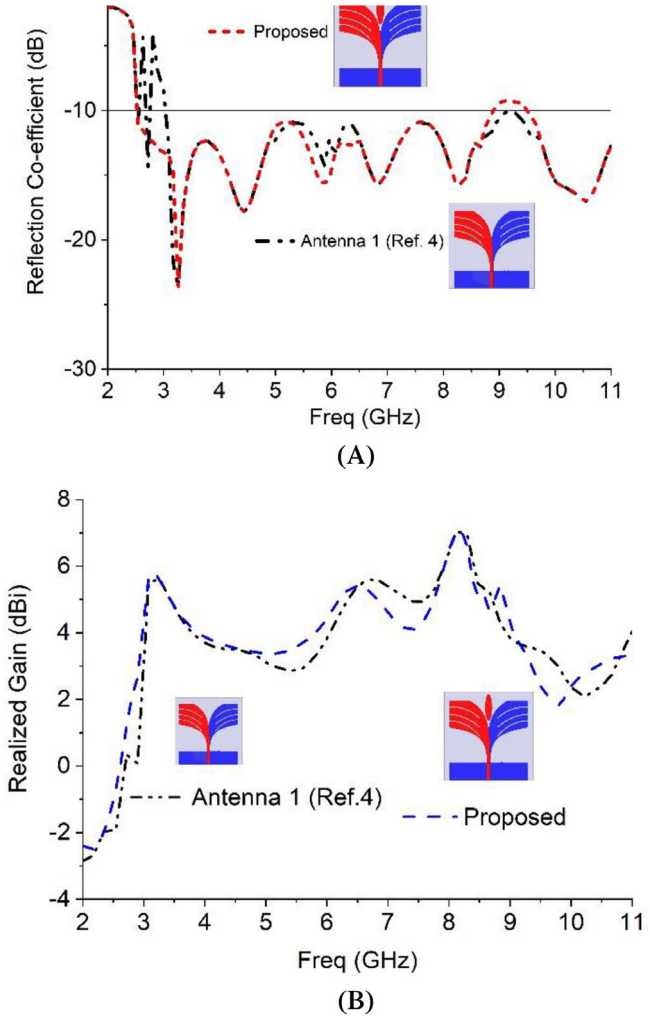


**FIGURE 3** A, Reflection coefficient ($S_{11}$) and B, peak realized a gain for Antenna1 (Ref. 4) and the proposed design with ellipse (Antenna2) [Color figure can be viewed at wileyonlinelibrary.com]

**TABLE 2** Different design modification results

| Changes in structure | Operating frequency range (GHz) | Fractional bandwidth (%) | Peak realized gain (dBi) |
|---|---|---|---|
| Antenna 1 (slotting fins) | 3.03-11 | 113 | 7.0 |
| Proposed design (antenna 2) | 2.50-11.00 | 125.92 | 7.2 |

dimensions $C_1$ in Figure 1C. An elliptical notch is placed at the top middle position of the patch. Afterward, the antenna results are being investigated. Finally, the satisfying results are obtained with the modification. Table 2 characterizes the valuations of the effects of antenna 1 (Ref. 4) and antenna 2 (proposed) on antenna performance. From Figure 3A,B, it can be observed that the proposed prototype has a wider BW compared to antenna 1(Ref 4. The antenna 1 with six fins slots in the top and bottom radiators, the lower

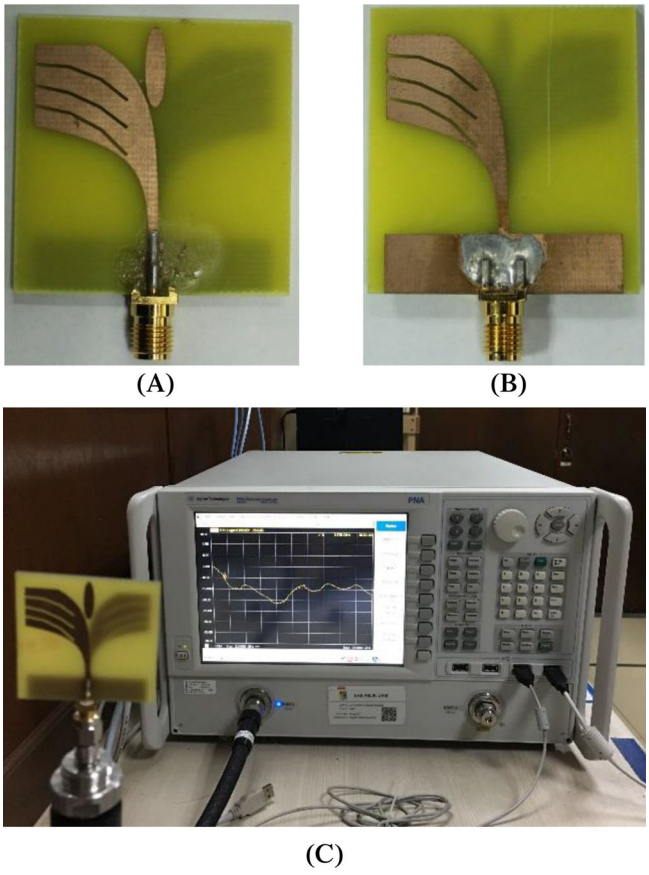


**FIGURE 4** The realized antenna. A, Front view. B, Back view. C, Measurement setup [Color figure can be viewed at wileyonlinelibrary.com]

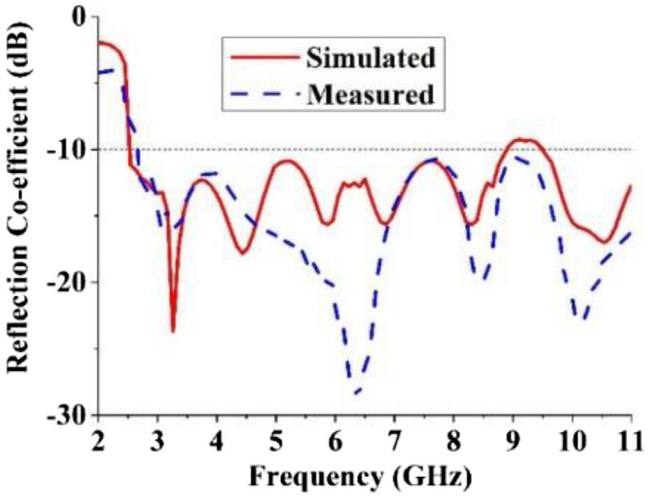


**FIGURE 5** The simulated and measured reflection coefficients ($S_{11}$) [Color figure can be viewed at wileyonlinelibrary.com]

frequency commenced at 3.03 GHz, and the higher frequency is shifted to 11 GHz. The proposed antenna with slots in fin and elliptical notch achieves a significant BW of 2.5 to above 11 GHz that covers the UWB band with maximum peak realized a gain of 7.2 dBi. The antenna touched a peak-realized gain of 7.2 dBi, while antenna 4 achieves the gain 6.1. The lower frequency gain is increased owing to the

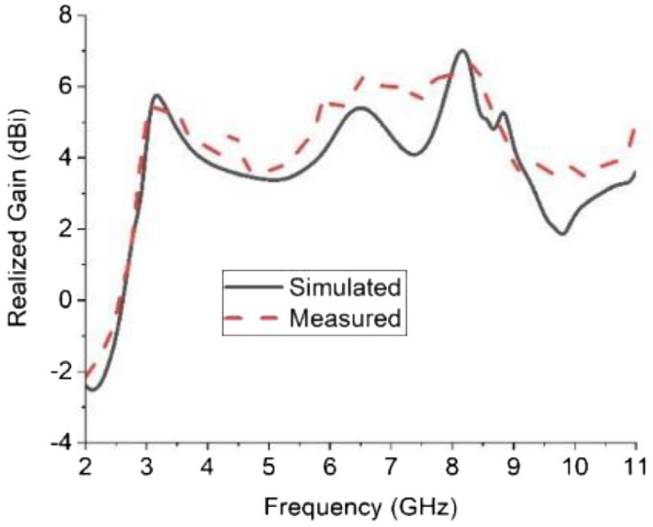


**FIGURE 6** The simulated and measured realized gain of the designed antenna [Color figure can be viewed at wileyonlinelibrary.com]

adjustment of the radiating aspects. The modifications in the radiator and the ellipse increase the electrical length that creates robust directive radiation owing to the overthrow of the surface current, which have vertical radiation at the end-fire path of the radiating fins.

## 3 | ANTENNA PERFORMANCE ANALYSIS

### 3.1 | Frequency domain characteristics

The antenna characteristics of the realized antenna have been designed, analyzed, and adjusted by using the computer simulation software (CST). The fabricated prototype and measurement setup are displayed in Figure 4. A PNA series vector network analyzer is used to measure the $S_{11}$ responses of the prototype. The measured and numerical reflection coefficient ($S_{11}$) curves of the antenna are presented in Figure 5. The antenna achieves an operating BW of 8.4 GHz

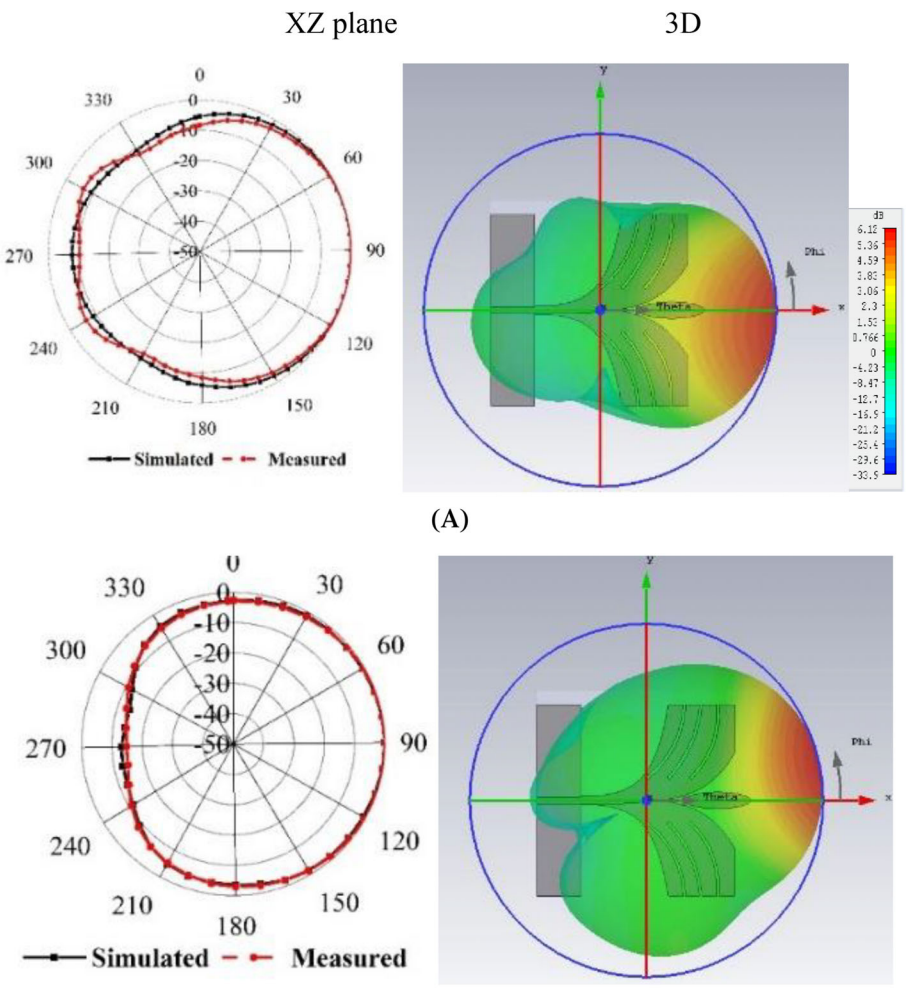


**FIGURE 7** The numerical and measured 2D and 3D radiation patterns: A, 3.30 GHz and B, 7.0 GHz [Color figure can be viewed at wileyonlinelibrary.com]

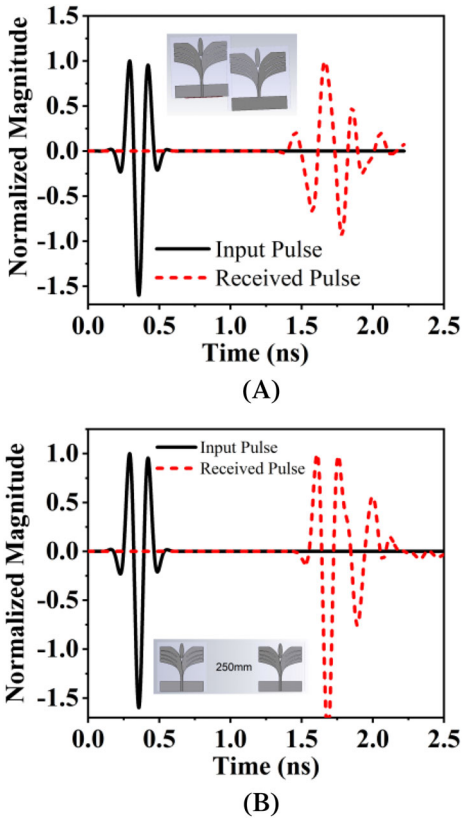


**FIGURE 8** Normalized magnitude. A, Face to face. B, side by side [Color figure can be viewed at wileyonlinelibrary.com]

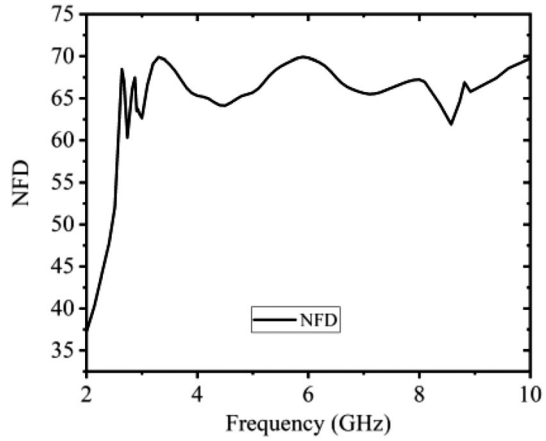


**FIGURE 9** NFD of the realized antenna. NFD, near-field directivity

(2.50-11 GHz). The first resonance is shifted to 2.5 GHz, and at 6.30 GHz the highest peak is observed several peaks through the band.

The simulated and measured realized gain is shown in Figure 6. The antenna has upward gain at the lower frequency range and stable to the higher frequency bands. The middling realized gain is recorded at 6 dBi accompanied by a maximum of 7.2 dBi at 8.30 GHz. The 2D (*XZ*-plane) and 3D radiation patterns are presented in Figure 7A,B for two frequencies of 3.30 and 70 GHz, respectively. It is observed in the near-field measurement; the antenna radiation is the end-fire direction, and the leading radiation direction is headed for the boresight.

### 3.2 | Time domain characteristics

The time domain performance of the antenna is displayed in Figure 8A,Bat two different setups of face-to-face and side-by-side (*X*-axis) at 200 mm distance. The waveforms are identical for transmitted and received signals at the f2f scenario. It proves that the antenna can transmit a short pulse with minimal alteration, except that the pulse spreads slightly. In the sbs direction, the transmitted and received magnitudes are not the same exactly. For the directional radiation features, the transmitted signal is a feast in a single track. For this, transmitted and received magnitudes are not of equal shape. The fidelity means the maximum magnitude of the cross-correlation between the transmitted and received pulses. For face-to-face orientation, the fidelity factor is 0.98, whereas for side by side it is 0.4479. The higher value of fidelity assures the lower falsification of the transmitted signal.

The near-field directivity (NFD) factor is the percentage of the power emitted inside the forward-facing side ($P_f$) and over the surface of the phantom ($P_T$), which can be calculated by the following equation:[26]

$$\mathrm{NFD} = \frac{Pf}{PT} \tag{4}$$

Figure 9 demonstrates the NFD of the antenna in the imaging setup. It is observed that near about 67% (average) of the total power is radiated through the front side of the breast tissue.

## 4 | IMAGING SETUP AND RESULTS

A breast phantom is used to test the 16-antenna array performance in detection of breast tumor through the CST simulation software, which is depicted in Figure 10A. The homogeneous phantom is constructed with four layers of skin, breast tissue, fat, and regular air layer. The skin layer width is 2.5 mm, and the dielectric constant is 38 with a conductivity of 1.49 S/m. The width of the breast tissue is 8.75 cm with a dielectric constant of 5.14 and 0.141 S/m of conductivity. The radius of the sphere tumor tissue is 1.8 mm with a dielectric constant of 67 and 49 S/m of conductivity. Figure 10B shows the skin, fat, and tumor dielectric constant vs frequency.[27,28] A 16-antenna array imaging setup is shown in Figure 10A, where the imaging setup consists of 16 wideband-modified Vivaldi antenna unit. The 8-antenna unit is placed vertically, and 8 antennas are placed horizontally surrounding the breast phantom with equal distance from each other. Among the 16 antennas, one antenna acts as a transmitter and rest of the 15 antennas act as a

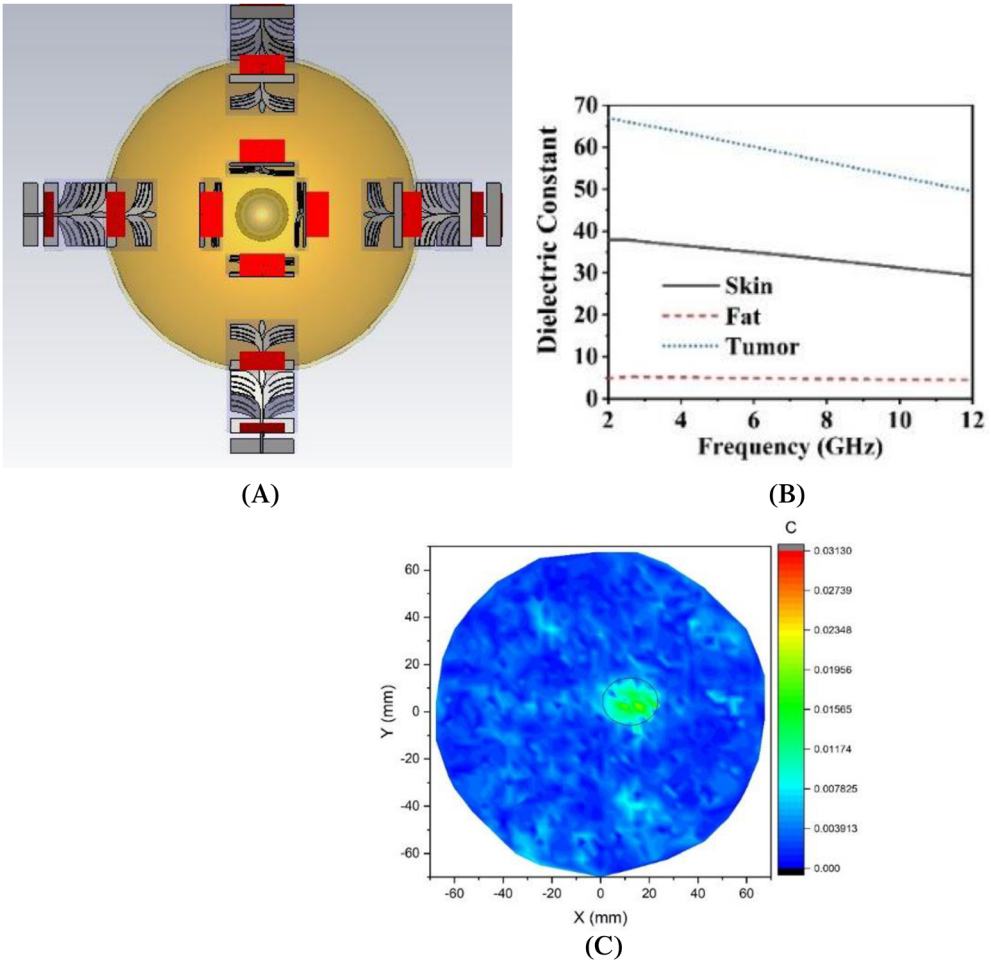


**FIGURE 10** Proposed model of breast phantom screening using A, 16-antenna unit. No. 1 is transmitting, and another 15 are receiving the signal. B, Skin, fat, and tumor dielectric constant vs frequency and C, Image of breast phantom with a tumor [Color figure can be viewed at wileyonlinelibrary.com]

**TABLE 3** Comparison of the performance with the reported antennas

| Ref. No. | Size ($mm^2$) $\lambda_0 \times \lambda_0$ | Operating bandwidth (GHz) | Gain (dBi) | Applications |
|---|---|---|---|---|
| 20 | 63 × 51<br>0.52 × 0.42 | 2.5-8.5 | 8.5 | Microwave breast imaging |
| 18 | 140 × 66<br>0.93 × 0.44 | 2-32 | 9 | Vivaldi antenna |
| 15 | 75 × 75<br>0.125 × 0.125 | 0.5-4.5 | 7 | Microwave radar imaging |
| 16 | 260 × 110<br>2.08 × 0.88 | 2.4-5.9 | 9 | Wireless communication |
| 19 | 40 × 50<br>0.27 × 0.33 | 2-12 | 5.2 | UWB |
| 30 | 100 × 53.19<br>0.66 × 0.35 | 2-27 | 7 | Microwave imaging |
| 31 | 124 × 100<br>1.07 × 0.86 | 2.6-11 | 6 | Vivaldi antenna |
| 31 | 135 × 100<br>1.35 × 1.0 | 3-12 | Not reported | UWB |
| 4 | 40 × 40<br>0.40 × 0.40 | 3.01-11 | 7.1 | Microwave breast imaging |
| Proposed | 40 × 40<br>0.40 × 0.40 | 2.5-11.00 | 7.2 | Microwave breast imaging |

receiver to receive the backscattered signal from the breast phantom. The process is repeated for each 16 antennas acting as a transmitter, and the total 240 ($16 \times 15$) scanned position has been considered for a complete breast phantom scan data set. The microwave propagates through the breast phantom tissues and backscattering signal from various tissue layers. After taking the data from the mentioned imaging setup, the backscattered signal data have been analyzed by using the MERIT open source software.[29] After processing the MERIT imaging toolbox, the imaging result has been presented in Figure 10C. It can be clearly stated that the tumor object has been clearly identified with a green color. This indicates that our system can be a good candidate for microwave imaging to detect the unwanted cell-like tumor through analyzing backscattering signal efficiently. A comparative study of reported antennas with the proposed one is listed in Table 3. The considered parameters are BW, dimension, antenna gain, and application. It can be noticed that the proposed antenna has a compact dimension, good gain, and wider bandwidth than the reported antennas.

## 5 | CONCLUSION

In this article, a compact, modified, and elliptical loaded antipodal Vivaldi antenna is designed and investigated for the breast tumor imaging application. The proposed antipodal Vivaldi antenna has modified by fins and loaded with an elliptical parasitic element for enhancing the impedance and directivity. The antenna has achieved 8.5 GHz bandwidth with a stable gain in the operating band. The antenna also shows excellent time domain performance (face-to-face and side-by-side) and NFD has been selected as a candidate for microwave imaging. An array of 16 antipodal antennas' setup imaging is designed where one antenna works as a transmitter and rest of the antenna works as a receiver in turn. The imaging performance is investigated with tumor tissue inside the breast phantom using the MERIT open source software. The analysis of imaging shows that the tumor is identified inside breast tissue from this imaging setup. Covering the modified antipodal Vivaldi antenna with time domain and frequency domain characteristics, the designed antenna can be a suitable candidate for early breast tumor detection through microwave imaging.

### ACKNOWLEDGMENT

This work is supported by Universiti Kebangsaan Malaysia research grant MI-2018-016.

### ORCID

*Md Samsuzzaman* https://orcid.org/0000-0002-1204-4858

### REFERENCES

[1] Islami F, Torre LA, Drope JM, Ward EM, Jemal A. Global cancer in women: cancer control priorities. *Cancer Epidemiol Biomarkers Prev*. 2017;26(4):458-470.

[2] Shao W, Edalati A, McCollough TR, McCollough WJ. A time-domain measurement system for uwb microwave imaging. *IEEE Trans Microw Theory Tech*. 2018;66(5):2265-2275.

[3] Abbak M, Akıncı M, Çayören M, Akduman I. Experimental microwave imaging with a novel corrugated Vivaldi antenna. *IEEE Trans Antennas Propag*. 2017;65(6):3302-3307.

[4] Islam M, Samsuzzaman M, Islam M, Kibria S, Singh MJS. A homogeneous breast phantom measurement system with an improved modified microwave imaging antenna sensor. *Sensors*. 2018;18(9):2962.

[5] Beada'a JM, Abbosh AM, Mustafa S, Ireland D. Microwave system for head imaging. *IEEE Trans Instrum Meas*. 2014;63(1):117.

[6] Porter E, Bahrami H, Santorelli A, Gosselin B, Rusch LA, Popović M. A wearable microwave antenna array for time-domain breast tumor screening. *IEEE Trans Med Imaging*. 2016;35(6):1501-1509.

[7] Islam MM, Islam MT, Faruque MRI, Samsuzzaman M, Misran N, Arshad H. Microwave imaging sensor using compact metamaterial uwb antenna with a high correlation factor. *Materials*. 2015;8(8):4631-4651.

[8] Sugitani T, Kubota S, Toya AXX, Kikkawa T. A compact 4x4 planar uwb antenna array for 3-d breast cancer detection. *IEEE Antennas Wirel Propag Lett*. 2013;12:733-736.

[9] Foroutan F, Nikolova NK. Active sensor for microwave tissue imaging with bias-switched arrays. *Sensors (Basel, Switzerland)*. 2018;18:E1447.

[10] Porter E, Kirshin E, Santorelli A, Coates M, Popovic M. Time-domain multistatic radar system for microwave breast screening. *IEEE Antennas Wireless Propag Lett*. 2013;12(1):229-232.

[11] Islam MT, Samsuzzaman M, Rahman M, Islam M. A compact slotted patch antenna for breast tumor detection. *Microw Opt Technol Lett*. 2018;60(7):1600-1608.

[12] Kibria S, Samsuzzaman M, Islam MT, Mahmud MZ, Misran N, Islam MT. Breast phantom imaging using iteratively corrected coherence factor delay and sum. *IEEE Access*. 2019;7:40822-40832.

[13] Moosazadeh M. High-gain antipodal Vivaldi antenna surrounded by dielectric for wideband applications. *IEEE Trans Antennas Propag*. 2018;66:4349-4352.

[14] McMillan R, Bohlander R. An investigation of millimeter wave propagation in the atmosphere: measurement program. Atlanta: Georgia Technology Research Institute, Georgia Institute of Technology; 1987.

[15] Wu B, Ji Y, Fang G. Design and measurement of compact tapered slot antenna for UWB microwave imaging radar, electronic measurement & instruments. Paper presented at: ICEMI'09. 9th International Conference on IEEE; 2009:222-229.

[16] He SH, Shan W, Fan C, Mo ZC, Yang FH, Chen JH. An improved Vivaldi antenna for vehicular wireless communication systems. *IEEE Antennas Wirel Propag Lett*. 2014;13:1505-1508.

[17] De Oliveira AM, Perotoni MB, Kofuji ST, Justo JF. A palm tree antipodal Vivaldi antenna with exponential slot edge for improved radiation pattern. *IEEE Antennas Wirel Propag Lett*. 2015;14:1334-1337.

[18] Nassar IT, Weller TM. A novel method for improving antipodal Vivaldi antenna performance. *IEEE Trans Antennas Propag*. 2015;63(7):3321-3324.

[19] Pandey G, Verma H, Meshram M. Compact antipodal Vivaldi antenna for UWB applications. *Electron Lett*. 2015;51(4):308-310.

[20] Abbak M, Çayören M, Akduman I. Microwave breast phantom measurements with a cavity-backed vivaldi antenna. *IET Microw Antenna P*. 2014;8(13):1127-1133.

[21] Biswas B, Ghatak R, Poddar D. A fern fractal leaf inspired wideband antipodal Vivaldi antenna for microwave imaging system. *IEEE Trans Antennas Propag*. 2017;65(11):6126-6129.

[22] Natarajan R, George JV, Kanagasabai M, Shrivastav AK. A compact antipodal Vivaldi antenna for UWB applications. *IEEE Antennas Wirel Propag Lett*. 2015;14:1557-1560.

[23] Guo L, Yang H, Zhang Q, Deng M. A compact antipodal tapered slot antenna with artificial material lens and reflector for gpr applications. *IEEE Access*. 2018;6:44244-44251.

[24] Greenberg MC, Virga KL. Characterization and design methodology for the dual exponentially tapered slot antenna. Paper presented at: Antennas and Propagation Society International Symposium, IEEE; 1999:88-91.

[25] Natarajan R, George JV, Kanagasabai M, et al. Modified antipodal vivaldi antenna for ultra-wideband communications. *IET Microw Antenna Propag*. 2016;10(4):401-405.

[26] Amineh RK, Trehan A, Nikolova NK. Tem horn antenna for ultra-wide band microwave breast imaging. *Prog Electromagn Res*. 2009;13:59-74.

[27] Mahmud MZ, Islam MT, Misran N, Kibria S, Samsuzzaman M. Microwave imaging for breast tumor detection using uniplanar amc based cpw-fed microstrip antenna. *IEEE Access*. 2018;6:44763-44775.

[28] Gabriel S, Lau R, Gabriel C. The dielectric properties of biological tissues: ii. Measurements in the frequency range 10 Hz to 20 GHz. *Phys Med Biol*. 1996;41(11):2251-2269.

[29] O'Loughlin D, Elahi MA, Porter E, et al. Open-Source Software for Microwave Radar-Based Image Reconstruction. Paper presented at: Proceedings of the 12th European Conference on Antennas and Propagation (EuCAP). London; 2018:9-13.

[30] Moosazadeh M, Kharkovsky S, Case JT, Samali B. Uwb antipodal Vivaldi antenna for microwave imaging of construction materials and structures. *Microw Opt Technol Lett*. 2017;59(6):1259-1264.

[31] Chamaani S, Mirtaheri SA, Abrishamian MS. Improvement of time and frequency domain performance of antipodal Vivaldi antenna using multi-objective particle swarm optimization. *IEEE Trans Antennas Propag*. 2011;59(5):1738-1742.

[32] Tianming L, Yuping R, Zhongxia N, Analysis and design of UWB Vivaldi antenna, microwave, antenna, propagation and EMC technologies for wireless communications. Paper presented at: International Symposium on IEEE; 2007:579-581.

**How to cite this article:** Samsuzzaman M, Islam MT, Islam MT, Shovon AAS, Faruque RI, Misran N. A 16-modified antipodal Vivaldi antenna array for microwave-based breast tumor imaging applications. *Microw Opt Technol Lett*. 2019;61:2110–2118. https://doi.org/10.1002/mop.31873